

Roles of High-lying Excited States on Neutrino Reactions and the Gamow Teller strength for ^{40}Ar

Eunja Ha and Myung-Ki Cheoun *

Department of Physics, Soongsil University, Seoul 156-743, Korea

(Dated: August 23, 2011)

Neutrino reactions on ^{40}Ar via charged and neutral currents for detecting solar and core collapsing supernovae (SNe) neutrinos and the Gamow Teller strength are calculated by considering the high-lying excited states up to a few tens of MeV region. The nucleus was originally exploited to identify the solar neutrino emitted from ^8B produced in the pp-chains on the Sun. With the higher energy neutrinos emitted from the core collapsing SNe, contributions from higher multi-pole transitions including the spin dipole resonances (SDR) as well as the Gamow Teller (GT) and Fermi transitions are shown to be important ingredients for understanding reactions induced by the SNe as well as solar neutrinos. In this work, we focused on the role of high-lying excited states which are located beyond a few low-lying states known in the experiment. Expected large difference between the cross sections of ν_e and $\bar{\nu}_e$ reactions on ^{40}Ar , which difference has been anticipated in previous calculations because of the large Q value in the $\bar{\nu}_e$ reaction, is significantly diminished. The reduction leads only to about 2 times difference between them. Our calculations are carried out by the Quasi-particle Random Phase Approximation (QRPA), which takes account of the neutron-proton pairing as well as proton-proton and neutron-neutron pairing correlations. They were successfully applied in the description of the nuclear beta decay and relevant neutrino reaction data on ^{12}C and ^{56}Fe , and the GT data on the ^{138}La and ^{180}Ta .

PACS numbers:

* Corresponding author : cheoun@ssu.ac.kr

I. INTRODUCTION

Neutrino reactions on ^{40}Ar were of astrophysical importance because they may be used to detect the solar neutrino emitted from ^8B via the pp-chains in the Sun. The reactions are measured through the liquid argon time projection chamber (LArTPC) at the ICARUS (Imaging of Cosmic and Rare Underground Signals) [1]. Since the maximum energy of the solar neutrino is thought to be about 17 MeV in the standard solar model, the neutrino reactions are naturally sensitive on the low-lying discrete energy states of ^{40}Ar .

Since the protons in ^{40}Ar are occupied mostly at the sd shell while the neutrons are located up to the pf shell, charge exchange reactions (CEX) on the nucleus are closely related to the multi-particle and multi-hole interactions of the both major shells. For instance, the Q-value for the $^{40}\text{Ar}(\nu_e, e^-)^{40}\text{K}^*$ reaction is 1.50 MeV, while the Q-value for the $^{40}\text{Ar}(\bar{\nu}_e, e^+)^{40}\text{Cl}^*$ reaction is 7.48 MeV, 5 times larger than the ν_e reaction. Therefore, $^{40}\text{Ar}(\bar{\nu}_e, e^+)^{40}\text{Cl}^*$ reactions might be kinematically disfavored in the low energy neutrino, such as solar neutrino, reactions. Moreover, in $^{40}\text{Cl}^*$, only 2 excited states for the Gamow Teller (GT) transition are known with no excited isobaric analogue states (ISB). In this respect, ^{40}Ar was thought to effectively distinguish the ν_e and $\bar{\nu}_e$ emitted from the Sun.

Recently, authors in Ref. [2] revised their previous works [3] in order to discuss the possible detection of neutrino oscillation of supernova (SN) neutrinos. The neutrinos emitted from the SN explosion can give valuable information about neutrino properties, such as the ν mixing angle θ_{13} and the mass hierarchy, because they traverse regions of dense matter in the exploding star where matter enhanced oscillations take place.

Here we briefly discuss such feasibility about how to extract such neutrino properties. One possible way is to investigate the abundances of light nuclei. Among the light nuclei, ^7Li and ^{11}B are abundantly produced through the ν -process (ν -induced reactions on related nuclei in the core collapsing supernova) [4–7]. Since the ν -induced reaction might be sensitive on the ν -properties as well as ν -flavors, the ^7Li and ^{11}B abundances could be sensitive on the ν parameters. For example, in Refs. [5, 8], the production yields of ^7Li and ^{11}B are shown to be sensitive on the neutrino mass hierarchy as well as the emitted neutrino temperature, although some other interpretations are still remained [9].

Another way is to directly detect the ν signals coming from the core collapsing SN explosion on the Earth [10]. The LArTPC was suggested as one of possibilities to enable

such detection. This ICARUS-like detector is also planned to detect the neutrino beam at CERN [11]. Since neutrino energies from the SN explosion are expected to have tens of MeV, which are higher than those stemmed from the solar neutrino [4, 5], one needs to consider the contributions from higher multi-pole transitions as well as high-lying excited states.

Refs. [2, 3] exploited the RPA calculation done by Kolbe and Langanke [12] and showed that contributions from higher multipoles, such as spin dipole resonances (SDR), could be important for the SN neutrino. The importance of higher multipole transitions is recently confirmed at the shell model (SM) calculation by Suzuki *et al.* [8] and also at the Quasi-particle Random Phase Approximation (QRPA) calculations by us [13–15].

Neutrino (ν) (antineutrino ($\bar{\nu}$)) energies and flux emitted from the core collapsing SN explosion are conjectured to be peaked from a few to tens of MeV energy region [4, 5, 16]. Therefore, the $\nu(\bar{\nu})$ -induced reactions on ^{40}Ar are sensitive on the high-lying excited states of the nucleus beyond one nucleon thresholds. One more point to be noticed is that the reaction proceeds via two-step processes, *i.e.* target nuclei are excited by incident $\nu(\bar{\nu})$ and decayed to lower energy states with the emission of some particles [12]. Of course, the one-step process, which directly knocks out one nucleon from a target nucleus with outgoing lepton, might work on the abundances of final nuclei [17]. In particular, the contribution could be comparable to that of the two-step process with the higher energy neutrino [18]. But, in this work, we do not take account of the effects by the one-step process.

The particle emission decay mode allows the daughter nuclei to easily proceed to adjacent nuclei and naturally influences the nuclear abundances in the universe. Since we do not have experimental data about the emission decay mode enough to fix relevant transitions, one usually resorts to the statistical model such as Hauser-Feshbach theory [8, 19, 20]. In this work, we take the approach done by Ref. [20]. Of course, the preceding excitation occurs through various transitions, *i.e.* super allowed Fermi ($J^\pi = 0^+$), allowed Gamow Teller (GT) ($J^\pi = 1^+$), SDR ($J^\pi = 0^-, 1^-, 2^-$), and other higher multipole transitions [8, 21].

Since our results for the SN neutrinos are briefly reported [22], in this work, we present more detailed and advanced results based on the QRPA calculation for $\nu(\bar{\nu})$ - ^{40}Ar reactions in the following two respects. The first point is that relevant cross sections for solar and SN neutrinos are calculated and compared simultaneously, whose energy ranges are considered up to 30 and 80 MeV region, respectively [16]. Secondly, we focus on roles of high-lying excited states around 20 MeV although they are not verified at the experiments. Our

results decrease the cross sections of $^{40}\text{Ar}(\nu_e, e^-)^{40}\text{K}^*$ reaction about 3.5 times and increase about twice those of $^{40}\text{Ar}(\bar{\nu}_e, e^+)^{40}\text{Cl}^*$ reaction compared to the previous calculations [2, 3]. Consequently, the expected 12 times difference between the reactions at $E_\nu = 80$ MeV is reduced drastically to about twice difference. The GT strength recently deduced from $^{40}\text{Ar}(\text{p}, \text{n})$ reactions [23], which is estimated to justify our calculations, is also reproduced in a satisfactory way.

In section II, our theoretical formalism is presented with the neutron-proton pairing correlations. Results of various neutrino induced reactions on ^{40}Ar are discussed at section III. Finally summaries and conclusion are given at section IV.

II. THEORETICAL FRAMEWORKS

Since our QRPA formalism for neutrino-nucleus ($\nu - A$) reactions is detailed at our previous papers [13, 14], here we summarize two important characteristics compared to other QRPA approaches. First, the Brueckner \mathcal{G} matrix is employed for two-body interactions inside nuclei by solving the following Bethe-Salpeter equation based on the Bonn CD potential for nucleon-nucleon interactions in free space

$$\mathcal{G}(w)_{ab,cd} = V_{ab,cd} + V_{ab,cd} \frac{Q_p}{w - H_0} \mathcal{G}(w)_{ab,cd} , \quad (1)$$

where a, b, c, d indicate the single nucleon basis states characterized by oscillator type wave functions with single particle energies from the Woods-Saxon potential. H_0 is the harmonic oscillator Hamiltonian and Q_p is the Pauli operator. $V_{ab,cd}$ is the phenomenological nucleon-nucleon potential in free space. It may enable us to reduce some ambiguities from nucleon-nucleon interactions inside nuclei.

Second, we include neutron-proton (np) pairing as well as neutron-neutron (nn) and proton-proton (pp) pairing correlations. In medium or medium-heavy nuclei, the np pairing contributes to some extent for relevant transitions because of small energy gaps between proton and neutron energy spaces [24]. Moreover the np pairing leads to a unified description of both charged current (CC) and neutral current (NC) reactions within a framework as shown later on.

But the contribution by the np pairing is shown to be only within $1 \sim 2$ % for the weak interaction in ^{12}C , such as β^\pm decay and the $\nu - ^{12}\text{C}$ reaction [13, 14], because the energy

gap between neutron and proton energy spaces is too large in such a light nucleus to be effective. But in medium-heavy nuclei, such as ^{56}Fe and ^{56}Ni , the np pairing effect accounts for 20 ~ 30 % of total cross sections [14]. Results by our QRPA have successfully described relevant ν -reaction data for ^{12}C [13], ^{56}Fe and ^{56}Ni [14], and ^{138}La and ^{180}Ta [15] as well as β , $2\nu\beta\beta$ and $0\nu2\beta\beta$ decays [24].

For CC reactions, the ground state of a target nucleus is described by the BCS vacua for the quasi-particle which comprises all types correlations. Excited states, $|m; J^\pi M\rangle$, in a compound nucleus are generated by operating the following one phonon operator to the initial nucleus

$$Q_{JM}^{+,m} = \sum_{kl\mu'\nu'} [X_{(k\mu'lv'J)}^m C^+(k\mu'lv'JM) - Y_{(k\mu'lv'J)}^m \tilde{C}(k\mu'lv'JM)] , \quad (2)$$

where pair creation operator C^+ is defined as

$$C^+(k\mu'lv'JM) = \sum_{m_k m_l} C_{j_k m_k j_l m_l}^{JM} a_{\nu'}^+ a_{k\mu'}^+ , \quad \tilde{C}(k\mu'lv'JM) = (-)^{J-M} C(k\mu'lv'J-M) \quad (3)$$

with a quasi-particle creation operator $a_{\nu'}^+$ and Clebsh-Gordan coefficient $C_{j_k m_k j_l m_l}^{JM}$. Here Roman letters indicate single particle states, and Greek letters with a prime mean quasi-particle types 1 or 2. If neutron-proton pairing is neglected, the phonon operator is easily decoupled to two phonon operators, charge changing and conserving reactions, as used in the usual proton-neutron QRPA (pnQRPA) [21]. The amplitudes $X_{\alpha\alpha',b\beta'}$ and $Y_{\alpha\alpha',b\beta'}$, which stand for forward and backward going amplitudes from ground states to excited states, are obtained from the QRPA equation [14, 24].

Under the second quantization, matrix elements of any transition operator $\hat{\mathcal{O}}$ between a ground state and an excited state $|\omega; JM\rangle$ can be factored as follows

$$\langle \omega; JM | \hat{\mathcal{O}}_\lambda | QRPA \rangle = [\lambda]^{-1} \sum_{ab} \langle a | \hat{\mathcal{O}}_\lambda | b \rangle \langle \omega; JM | [c_a^+ \tilde{c}_b]_\lambda | QRPA \rangle , \quad (4)$$

where c_a^+ is the creation operator of a real particle at state a . The first factor $\langle a | \hat{\mathcal{O}}_\lambda | b \rangle$ can be calculated for a given single particle basis independently of the nuclear model [25, 26]. By using the phonon operator $Q_{JM}^{+,m}$, we obtain the following expressions for CC and NC

neutrino reactions

$$\begin{aligned}
& < \omega; JM || \hat{\mathcal{O}}_\lambda || QRPA >_{CC} \\
& = \sum_{a\alpha' b\beta'} [\mathcal{N}_{a\alpha' b\beta'} < a\alpha' || \hat{\mathcal{O}}_\lambda || b\beta' > [u_{pa\alpha'} v_{nb\beta'} X_{a\alpha' b\beta'} + v_{pa\alpha'} u_{nb\beta'} Y_{a\alpha' b\beta'}] , \\
& < \omega; JM || \hat{\mathcal{O}}_\lambda || QRPA >_{NC} \\
& = \sum_{a\alpha' b\beta'} [\mathcal{N}_{a\alpha' b\beta'} < a\alpha' || \hat{\mathcal{O}}_\lambda || b\beta' > [u_{pa\alpha'} v_{pb\beta'} X_{a\alpha' b\beta'} + v_{pa\alpha'} u_{pb\beta'} Y_{a\alpha' b\beta'}] \\
& \quad - (-)^{j_a + j_b + J} \mathcal{N}_{b\beta' a\alpha'} < b\beta' || \hat{\mathcal{O}}_\lambda || a\alpha' > [u_{pb\beta'} v_{pa\alpha'} X_{a\alpha' b\beta'} + v_{pb\beta'} u_{pa\alpha'} Y_{a\alpha' b\beta'}]] + (p \rightarrow n) ,
\end{aligned} \tag{5}$$

where $\mathcal{N}_{a\alpha' b\beta'}(J) = \sqrt{1 + \delta_{ab} \delta_{\alpha'\beta'} (-1)^J / (1 + \delta_{ab} \delta_{\alpha'\beta'})}$. By switching off the np pairing, these forms are also easily reduced to the result by the pnQRPA [21]

The weak current operators, $\hat{\mathcal{O}}_\lambda$, composed of longitudinal, Coulomb, electric and magnetic operators, are detailed at Ref. [14]. Finally, based on initial and final nuclear states, cross section for $\nu(\bar{\nu})$ reactions through the weak transition operator is given as [26]

$$\begin{aligned}
\left(\frac{d\sigma_\nu}{d\Omega} \right)_{(\nu/\bar{\nu})} &= \frac{G_F^2 \epsilon k}{\pi (2J_i + 1)} \left[\sum_{J=0} (1 + \vec{\nu} \cdot \vec{\beta}) | < J_f || \hat{\mathcal{M}}_J || J_i > |^2 \right. \\
&+ (1 - \vec{\nu} \cdot \vec{\beta} + 2(\hat{\nu} \cdot \hat{q})(\hat{q} \cdot \vec{\beta})) | < J_f || \hat{\mathcal{L}}_J || J_i > |^2 - \\
&\hat{q} \cdot (\hat{\nu} + \vec{\beta}) 2 \text{Re} < J_f || \hat{\mathcal{L}}_J || J_i > < J_f || \hat{\mathcal{M}}_J || J_i >^* \\
&+ \sum_{J=1} (1 - (\hat{\nu} \cdot \hat{q})(\hat{q} \cdot \vec{\beta})) (| < J_f || \hat{\mathcal{T}}_J^{el} || J_i > |^2 + | < J_f || \hat{\mathcal{T}}_J^{mag} || J_i > |^2) \\
&\left. \pm \sum_{J=1} \hat{q} \cdot (\hat{\nu} - \vec{\beta}) 2 \text{Re} [< J_f || \hat{\mathcal{T}}_J^{mag} || J_i > < J_f || \hat{\mathcal{T}}_J^{el} || J_i >^*] \right] ,
\end{aligned} \tag{6}$$

where (\pm) means the case of $\nu(\bar{\nu})$, respectively. $\vec{\nu}$ and \vec{k} are incident and final lepton 3-momenta, $\vec{q} = \vec{k} - \vec{\nu}$ and $\vec{\beta} = \vec{k}/\epsilon$ with the final lepton's energy ϵ .

For CC reactions we multiplied Cabbibo angle $\cos^2 \theta_c$ and considered the Coulomb distortion of outgoing leptons in a residual nucleus [8, 21]. By following the prescriptions on Refs.[12, 21], we choose an energy point in which both approaches predict same values. Then we use the Fermi function below the energy and the effective momentum approach (EMA) above the energy.

Our QRPA includes not only proton-proton and neutron-neutron pairing but also neutron-proton (np) pairing correlations. The np pairing is included at the BCS stage to reproduce empirical np pairing gaps by adjusting a renormalized strength parameter g_{np} embedded in the Brueckner G matrix in the following theoretical pairing gap [24]

$$\delta_{np} = -[(H'_0 + E'_1 + E'_2) - (H_0 + E_1 + E_2)], \tag{7}$$

where $H'_0(H_0)$ is total ground state energy with (without) np pairing and $E'_1 + E'_2$ ($E_1 + E_2$) is a sum of the lowest two quasi-particles energies with (without) np pairing correlations. More detailed procedures for the inclusion of the np pairing correlations are presented at Refs. [15, 24].

III. RESULTS

A. Neutrino reactions on ^{40}Ar via charged current

In Fig.1, we show results for CC reactions, $^{40}\text{Ar}(\nu_e, e^-)^{40}\text{K}^*$ for solar and SN neutrinos. For solar neutrinos (upper part), cross sections are fully ascribed to the the GT and Fermi transitions. Other transitions contribute only a few % to the cross section below 30 MeV region. Since the maximum energy of the solar neutrino from ^8B is believed to be 12 MeV, solar neutrino reactions are dominated by the GT and Fermi transitions.

These results justify previous SM calculations for solar neutrino reactions on ^{40}Ar [27, 31], which consider only the GT and Fermi transitions. The phenomenological approach $\sigma = 3\sigma_{Fermi}$ used at Ref. [16] is approximately good on the energy region above 20 MeV, but $\sigma = 2\sigma_{Fermi}$ is much better below 20 MeV region.

But for SN neutrinos (lower part), contributions from the spin dipole resonance (SDR) (1^- and 2^-) are increased to those by the Fermi transition around 55 MeV and becomes larger about $2 \sim 2.5$ times of the Fermi transition beyond the region. Other higher multipole transitions, ($2^\pm, 3^\pm$ and 4^\pm) contribute 10 % maximally. Of course, both GT and Fermi transitions are still main components. For example, their contributions are $70 \sim 80$ % around 50 MeV region, and $60 \sim 50$ % above 50 MeV region. These phenomena, the dominance of the GT and Fermi transitions, are typical of CC reactions on even-even nuclei, for example, ^{12}C , ^{56}Fe and ^{56}Ni [13, 14].

Our cross sections in Fig. 1 are smaller on the whole energy region about 3.5 times rather than previous RPA calculations [2]. In the following the characteristics of both approaches are explained with the reason why we predict such small cross sections. We include excited states of $^{40}\text{K}^*$ up to a few tens of MeV, which are generated by the phonon operator in Eq.(2), while the RPA calculation [2, 3] seems to take only a few excited states known in the experiment.

But the high-lying excited states affect phase space in Eq. (6) through the energy conservation, $\epsilon = E_\nu - \omega$, with the outgoing lepton energy ϵ , the incident neutrino energy E_ν and the energy transfer ω . Energy transfer to the target nucleus ω , which just corresponds to the excited energy, makes the energy of outgoing electrons ϵ in Eq. (6) smaller than that of incident neutrino energy. It leads to the smaller cross sections because the increase rate of transition strengths cannot follow the decrease of the phase space.

If we take the few known states, the cross sections are easily increased to match well with the RPA calculation simply because of the increase of the outgoing lepton energy in Eq.(6). Excited states beyond the known states decrease cross sections even for the solar neutrino case. Recent calculation of $^{40}\text{Ar}(\nu, e^-)$ by the local density approximation shows also such a tendency because it does not also include discrete states explicitly [28].

B. Gamow Teller strength by ^{40}Ar (p,n) reactions

In Fig. 2, we show the GT(\pm) strength distributions and their running sums, whose excitations energies are with respect to the ground state of ^{40}Ar . The higher energy states we go to, the larger strength and their running sums are obtained. In specific, discrete energy states on the 10 \sim 20 MeV region affect significantly the neutrino reaction. Even for solar neutrinos, these energy states reduce cross sections compared to those calculated by a few known states.

Very recently, the GT strength up to 8 MeV are extracted from $^{40}\text{Ar}(\text{p,n})$ reactions [23]. Consistency of our results with the experimental GT($-$) strength can be shown by studying the strength distribution and its running sum in the lower energy states at Fig.2. The GT strength of ours are localized at 3.6, 3.7, 8.6 and 8.9 MeV from the ^{40}Ar ground state, which corresponds to 2.1, 2.2, 7.1 and 7.4 MeV from the ^{40}K ground state. They are consistent with the data by the $^{40}\text{Ar}(\text{p,n})$ reaction [23], apart from their strength, although some minor states between 2 and 7 MeV energy region are not verified in detail in our calculations. But its running sum up to 7.5 MeV from ^{40}K ground state, whose value is $\Sigma B(\text{GT}_-) = 4 \sim 5$, is nicely reproduced in our approach by multiplying the $(g_V/g_A)^2$ to our results $\Sigma B(\text{GT}_-) = 3.6$. The GT strength derived by our QRPA is thought to be reliable enough to justify our conjecture on the role of higher excited states.

Based on the GT and Fermi strength distributions, Bhattacharya *et al.* [23] deduced ν_e

reactions on ^{40}Ar up to 30 MeV in the following way

$$\sigma(E_\nu) = \frac{G_F^2 \cos^2 \theta_c}{\pi \hbar^4 c^3} \sum_i k_i \epsilon_i F(Z, \epsilon_i) [B_i(GT) + B_i(F)] , \quad (8)$$

where k_i and ϵ_i refer to the momentum and total energy of the outgoing electron and $F(Z, \epsilon_i)$ accounts for the Coulomb correction. They are shown to be consistent with those by the β decay on the mirror nucleus, ^{40}Ti [29, 30]. The neutrino cross sections of $^{40}\text{Ar}(\nu, e^-)$ obtained by Eq.(8) were very similar to the previous results calculated by a few experimental excited states [2] around a few MeV region. For example, the cross section around 30 MeV region is about $200 \times 10^{-42} \text{cm}^2$, which is about 3 times larger than our prediction at Fig.1. Since the excited states newly verified in the $^{40}\text{Ar}(p, n)$ reaction are also located on the energy region below 10 MeV, deduced cross sections are rarely affected by the new GT strength data.

It should be noted that Eq. (8) is valid only near threshold of the outgoing electron as commented at Ref. [23]. For example, one can obtain very easily Eq. (8) from Eq. (6), which is exact form for the cross section, by putting the 3-momentum of the outgoing electron $\vec{k} = 0$ and considering only $J = 0$ and 1 for the Fermi and the GT transitions, respectively. Therefore, Eq. (8) cannot be applied for the incident neutrino energy beyond the electron threshold considered in this report.

C. Anti-neutrino reactions on ^{40}Ar via charged current

This reduction of cross sections by the higher excited states should function on the $\bar{\nu}_e$ reaction, $^{40}\text{Ar}(\bar{\nu}_e, e^+)^{40}\text{Cl}^*$. Fig. 3 shows results for $^{40}\text{Ar}(\bar{\nu}_e, e^+)^{40}\text{Cl}^*$ via CC for solar and SN neutrinos. General trends of the GT, Fermi and SDR transitions are very similar to the results of $^{40}\text{Ar}(\nu_e, e^-)^{40}\text{K}^*$. For solar neutrinos, the GT and Fermi transitions are main components, but the SDR (1^- and 2^-) contributions emerge largely for the SNe neutrinos. Cross sections for solar $\bar{\nu}_e$ are almost same as the those by the ν_e reaction, $^{40}\text{Ar}(\nu_e, e^-)^{40}\text{K}^*$, while they are about a half of those by the ν_e reaction for SN neutrinos.

This is contrast to the results of Refs. [2, 3]. Actually, they addressed about 12 times difference between the ν_e and $\bar{\nu}_e$ reactions in the cross section at $E_\nu = 80$ MeV. Since the Q value for the $\bar{\nu}_e$ reaction, 7.48 MeV, decreases the incident neutrino energy by the Q value, *i.e.* as $E_\nu^i \rightarrow E_\nu^i - Q = \epsilon + \omega$, the reaction is disfavored by the low energy neutrino. Consequently, it may play a role of reducing the $\bar{\nu}_e$ cross section for a given energy. The

strong reduction of cross sections for the $\bar{\nu}_e$ reaction by the large Q value was one of the motivation to distinguish the ν_e and $\bar{\nu}_e$ reactions on ^{40}Ar target.

However, the high-lying excited states weaken the decrease of cross sections by the Q value, so that the expected large decrease of cross sections by the Q value is not so drastic compared to those by a few known excited states. As a result, our cross sections by $\bar{\nu}_e$ are about twice larger than those of Refs. [2, 3]. Since the cross sections by ν_e become smaller about 3.5 times than those by previous calculations, total difference between the ν_e and $\bar{\nu}_e$ reactions turns out to be only $2 \sim 3$ times difference. Higher excited states are directly associated to the reason why we have only about twice difference at $E_\nu = 80$ MeV between the ν_e and $\bar{\nu}_e$ reactions.

In general, $\bar{\nu}_e$ cross sections up to around a few tens MeV region are nearly same as those by ν_e , if we investigate results for other nuclei. Actually, the difference between $\bar{\nu}_e$ -A and ν_e -A reactions is given by the last term in Eq.(6), the interference term of magnetic and electric transitions. It means that main interactions for ν - ^{40}Ar stem from the longitudinal and Coulomb transitions. Nuclear effects such as the Q value are not so large as to give rise to such a large difference, if we consider the higher excited states.

Fermi function for the Coulomb correction is used on the energy region below 40 MeV and the effective momentum approach (EMA) is taken beyond 40 MeV. Coulomb corrections do not affect the difference between $\bar{\nu}_e$ -A and ν_e -A reactions. Both reactions are increased by about 15 % maximally by the Coulomb distortion. For pairing interactions, $g_{nn} = 1.105$, $g_{pp} = 1.057$ and $g_{np} = 1.5368$ are used to reproduce the empirical pairing gaps $\Delta_{nn} = 1.768$, $\Delta_{pp} = 1.776$ and $\delta_{np} = 0.684$ MeV for ^{40}Ar , respectively [24].

D. Neutrino and anti-neutrino reactions on ^{40}Ar via neutral current

Figs.4 and 5 shows results for NC reactions $^{40}\text{Ar}(\nu_e, \nu_e)^{40}\text{Ar}^*$ and $^{40}\text{Ar}(\bar{\nu}_e, \bar{\nu}_e)^{40}\text{Ar}^*$ for solar and SN neutrinos. They are dominated by the GT transition for solar neutrinos, which accounts for about a half of cross sections for SN neutrinos. It is typical of the NC reaction on even-even nuclei [13, 14]. Cross sections presented here are smaller than those used in Refs. [2, 3] because of the roles of higher energy states discussed for the CC reactions. One more point to be noticed is that our calculations for CC and NC reactions are carried out by a framework as shown in Eqs. (2) and (5). All of results are summarized in Fig.6 by

the logarithm to grasp whole neutrino reactions on ^{40}Ar . Cross sections by the CC are 4 \sim 5 times larger than those by the NC reaction

IV. SUMMARIES AND CONCLUSION

We calculated neutrino induced reactions on ^{40}Ar by including multipole transitions up to $J^\pi = 4^\pm$ with explicit momentum dependence. Our QRPA includes neutron-proton (np) pairing as well as neutron-neutron and proton-proton pairing correlations. Since energy gaps between proton and neutron energy spaces in medium nuclei are adjacent to each other, the np pairing may affect significantly the nuclear weak interaction.

In this work, we take account of excited states up to a few tens of MeV in contrast to the previous RPA calculations, which consider only a few known states in the experiment. These excited states, in specific, located on 10 \sim 20 MeV region reduce strongly corresponding cross sections and weaken the decrease of the cross sections by the Q value in the $\bar{\nu}_e$ reaction.

The amount of the increase of cross sections in our results is smaller than that by previous calculations. They consider only low-lying states and maybe treat the neglected high-lying states as elastic channels, which leads to such large cross sections. Contributions by the elastic channels in high-lying states in previous calculations, which are usually larger than inelastic channels, for example, the quasi-elastic peak, are compensated by the explicit contribution owing to the inelastic channels coming from the high-lying states.

By these higher excited states, the large Q value for $^{40}\text{Ar}(\bar{\nu}_e, e^+)^{40}\text{Cl}^*$ reaction, which motivated discerning ν_e and $\bar{\nu}_e$ reactions on ^{40}Ar , does not give rise to such a drastic difference about 12 times, but it leads to about 2 times difference between both reactions. More experimental data for higher excited states through relevant experiments are necessary for further discussion and conclusion for the difference. Study of the GT transition by (^3He , t) or (p,n) reactions could be viable approaches for obtaining the data [32].

^{40}Ar has a difficulty of considering two different major shells, *sd* and *fp*, which cause large number configurations with multi-particle and multi-hole interactions. The QRPA is a very efficient method to consider such multi-particle and multi-hole interactions and their configuration mixing, and successfully described the nuclear weak reactions sensitive on the nuclear structure, such as various β decays and relevant neutrino-nucleus reactions. Therefore our QRPA results for the $\nu_e(\bar{\nu}_e)-^{40}\text{Ar}$ reaction could be a useful reference for the

detection of SN neutrinos in the LArTPC detector.

Possible deformation in the exotic nuclei of astrophysical importance might be dealt with the Deformed QRPA (DQRPA) [33], which explicitly takes the deformation into account in the deformed Nilsson basis. Preliminary results on the GT strength distribution by the DQRPA show the importance of the deformation for understanding the neutrino induced reactions on the unstable nuclei [34].

This work was supported by the National Research Foundation of Korea (2011-0015467) and one of author, Cheoun, was supported by the Soongsil University Research Fund.

-
- [1] A. Rubbia, Nucl. Phys. **B 66**, 436 (1998).
 - [2] I. Gil-Botella and A. Rubbia, arXiv:hep-ph/0307244v2, Revised Feb.7, (2008).
 - [3] I. Gil-Botella and A. Rubbia, J. of Cosmology and Astroparticle Physics, **10**, 009 (2003).
 - [4] S. E. Woosley, D. H. Hartmann, R. D. Hoffmann, and W. C. Haxton, Astrophys. J. **356**, 272 (1990).
 - [5] T. Yoshida, T. Suzuki, S. Chiba, T. Kajino, H. Yokomukura, K. Kimura, A. Takamura, H. Hartmann, Astro. Phys. J. **686**, 448 (2008).
 - [6] A. Heger E. Kolbe, W.C. Haxton, K. Langanke, G. Martínez-Pinedo, S.E. Woosley, Phys. Lett. **B606**, 258 (2005).
 - [7] T. Suzuki, M. Honma, K. Higashiyama, T. Yoshida, T. Kajino, T. Otsuka, H. Umeda, and K. Nomoto, Phys. Rev. C **79**, 061603(R) (2009).
 - [8] T. Suzuki, S. Chiba, T. Yoshida, T. Kajino, T. Otsuka, Phys. Rev. C **74**, 034307 (2006).
 - [9] Myung-Ki Cheoun, T. Kajino, M. Kusagabe, Grant J. Mathews, Phys. Rev. D **84**, 043001 (2011).
 - [10] A. S. Dighe and A. Y. Smirnov, Phys. Rev. **D 62**, 033007 (2000).
 - [11] A. Curioni, Nucl. Phys. **B 159**, 69 (2006).
 - [12] E. Kolbe, K. Langanke, G. Martinez-Pinedo and P. Vogel, J. Phys. G **29**, 2569 (2003).
 - [13] Myung-Ki Cheoun, Eunja Ha, S. Y. Lee, W. So, K. S. Kim and T. Kajino, Phys. Rev. **C 81**, 028501 (2010).
 - [14] Myung-Ki Cheoun, Eunja Ha, K. S. Kim and T. Kajino, J. of Phys. **G 37**, 055101, (2010).

- [15] Myung-Ki Cheoun, Eunja Ha, T. Hayakawa, S. Chiba and T. Kajino, Phys. Rev. **C 82**, 035504, (2010).
- [16] Todd A. Thompson, Adam Burrows, Philip A. Pinto, Astrophys. J. **592**, 434 (2003).
- [17] K. S. Kim and Myung-Ki Cheoun, Phys. Lett. **B 679**, 330 (2009).
- [18] Myung-Ki Cheoun and K. S. Kim, J. of the Phys. Soc. of Japan **78**, 084202 (2009).
- [19] W. Hauser and H. Feshbach, Phys. Rev. **87**, 366 (1952).
- [20] T. Nakagawa, S. Chiba, T. Hayakawa, T. Kajino, Atomic Data and Nuclear Data Table, **91**, 77, (2005).
- [21] N. Paar, D. Vretenar, T. Marketin, and P. Ring, Phys. Rev. **C 77**, 024608 (2008).
- [22] Myung-Ki Cheoun, Eunja Ha and T. Kajino, Phys. Rev. **C 83**, 028801, (2011).
- [23] M. Bhattacharya, C. D. Goodman, and A. Garcia, Phys. Rev. **C 80**, 055501 (2009).
- [24] M. K. Cheoun, A. Bobyk, Amand Faessler, F. Simcovic and G. Teneva, Nucl. Phys. **A561**, 74 (1993) ; Nucl. Phys. **A564**, 329 (1993); M. K. Cheoun, G. Teneva and Amand Faessler, Prog. Part. Nuc. Phys. **32**, 315 (1994) ; M. K. Cheoun, G. Teneva and Amand Faessler, Nucl. Phys. **A587**, 301 (1995).
- [25] T. W. Donnelly and W. C. Haxton, ATOMIC DATA AND NUCLEAR DATA **23**, 103 (1979).
- [26] J. D. Walecka, *Muon Physics*, edited by V. H. Huges and C. S. Wu (Academic, New York, 1975), Vol II.
- [27] E. K. Warburton, Phys. Rev. **C 44**, 268 (1991).
- [28] M. S. Athar, S. Ahmad, S. K. Singh, Nucl. Phys. **A 764**, 551 (2006).
- [29] W. Trinder *et al.*, Phys. Lett. **B 415**, 211 (1997).
- [30] M. Bhattacharya *et al.*, Phys. Rev. **C 58**, 3677 (1998).
- [31] W. E. Ormand, P. M. Puzzochoero, P. F. Bortignon, R. A. Broglia, Phys. Lett. **345**, 343 (1995).
- [32] Y. Shimbara *et al.*, *The 10th International Symposium on Origin of Matter and Evolution of Galaxies*, edited by I. Tanihara *et. al.*, AIP, New York, 201 (2010).
- [33] M. S. Yousef, V. Rodin, A. Faessler, and F. Simkovic, Phys. Rev. **C 79**, 014314 (2009).
- [34] Eunja Ha and Myung-Ki Cheoun, *The 10th International Symposium on Origin of Matter and Evolution of Galaxies*, edited by I. Tanihara *et. al.*, AIP, New York, 351 (2010).

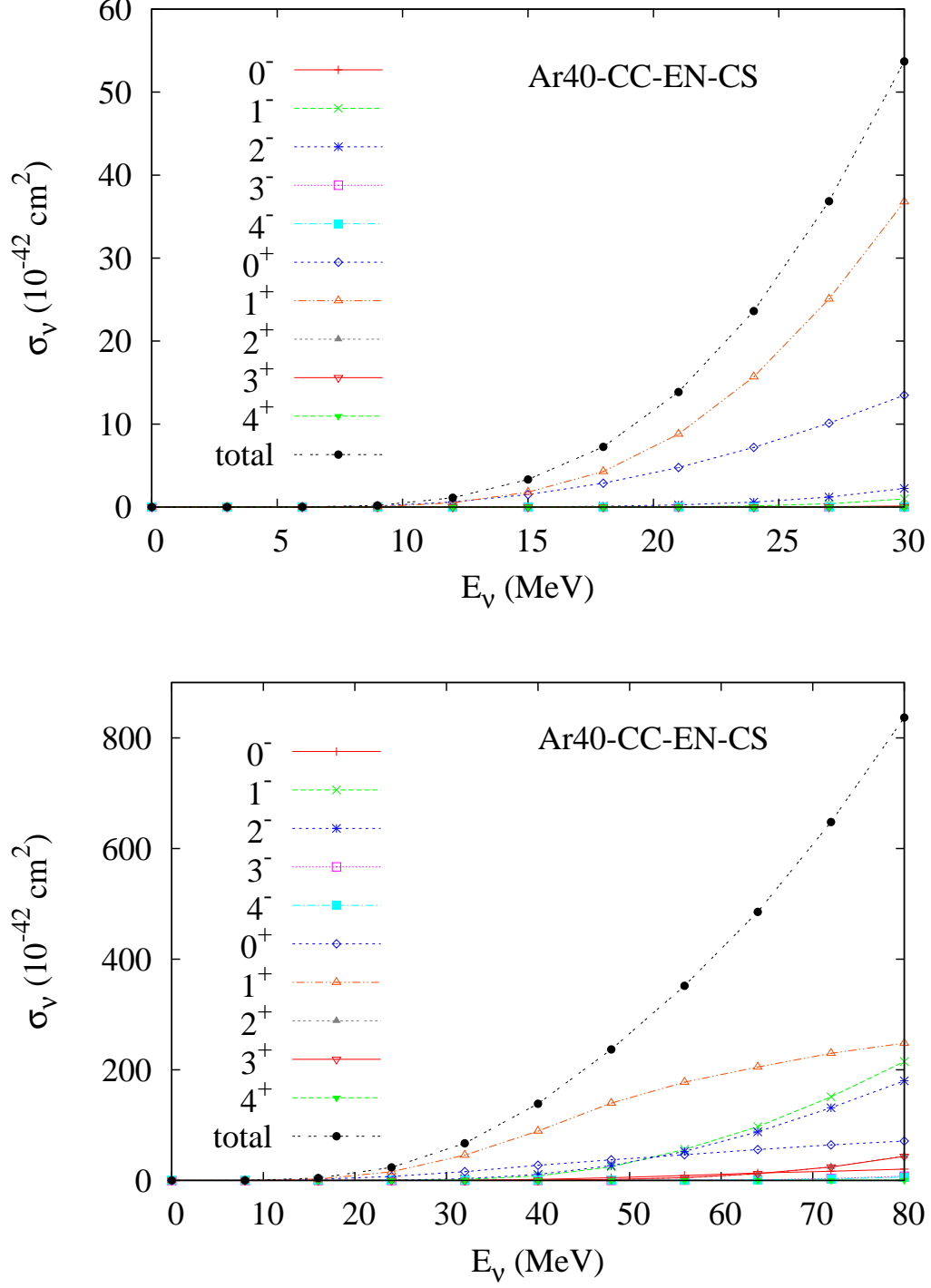


FIG. 1: (Color online) Cross sections by charged current, $^{40}\text{Ar}(\nu_e, e^-)^{40}\text{K}^*$ for solar (upper) and SN (lower) neutrinos. For solar (supernova) neutrinos, the $E_{\nu_e}^{max.} = 30(80)$ MeV are used for $J_\pi = 0^\pm \sim 4^\pm$ states.

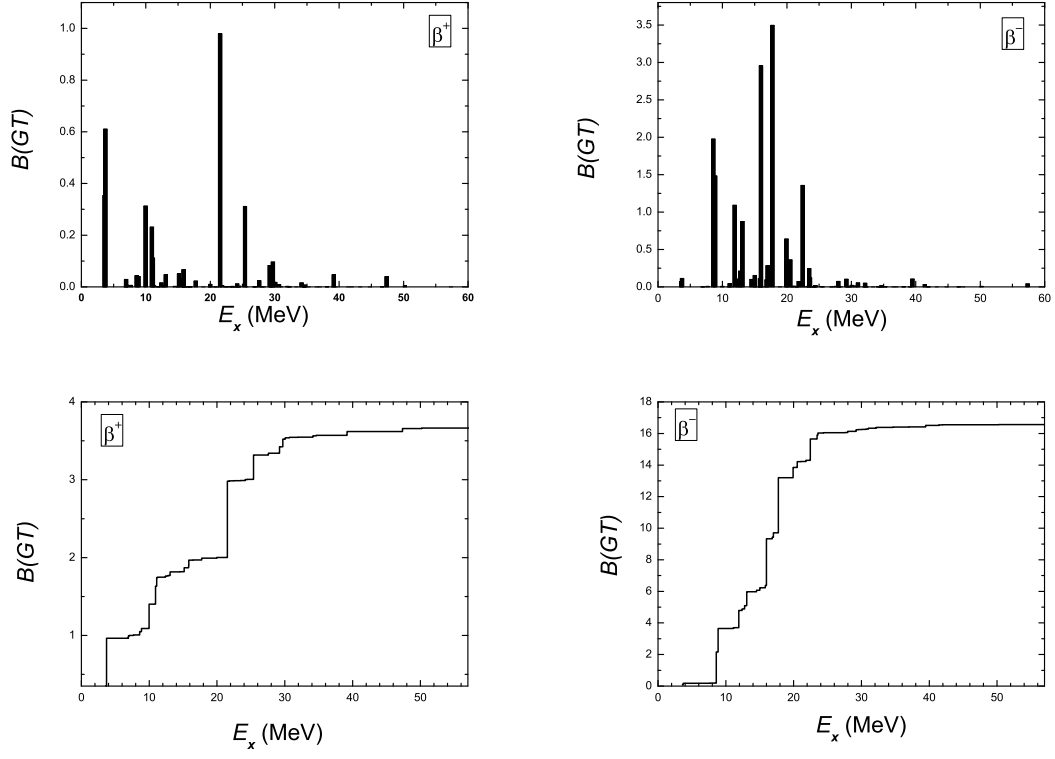


FIG. 2: The Gamow Teller strength $GT(\pm)$ from ^{40}Ar and their running sums. E_x is with respect to the ground state of ^{40}Ar .

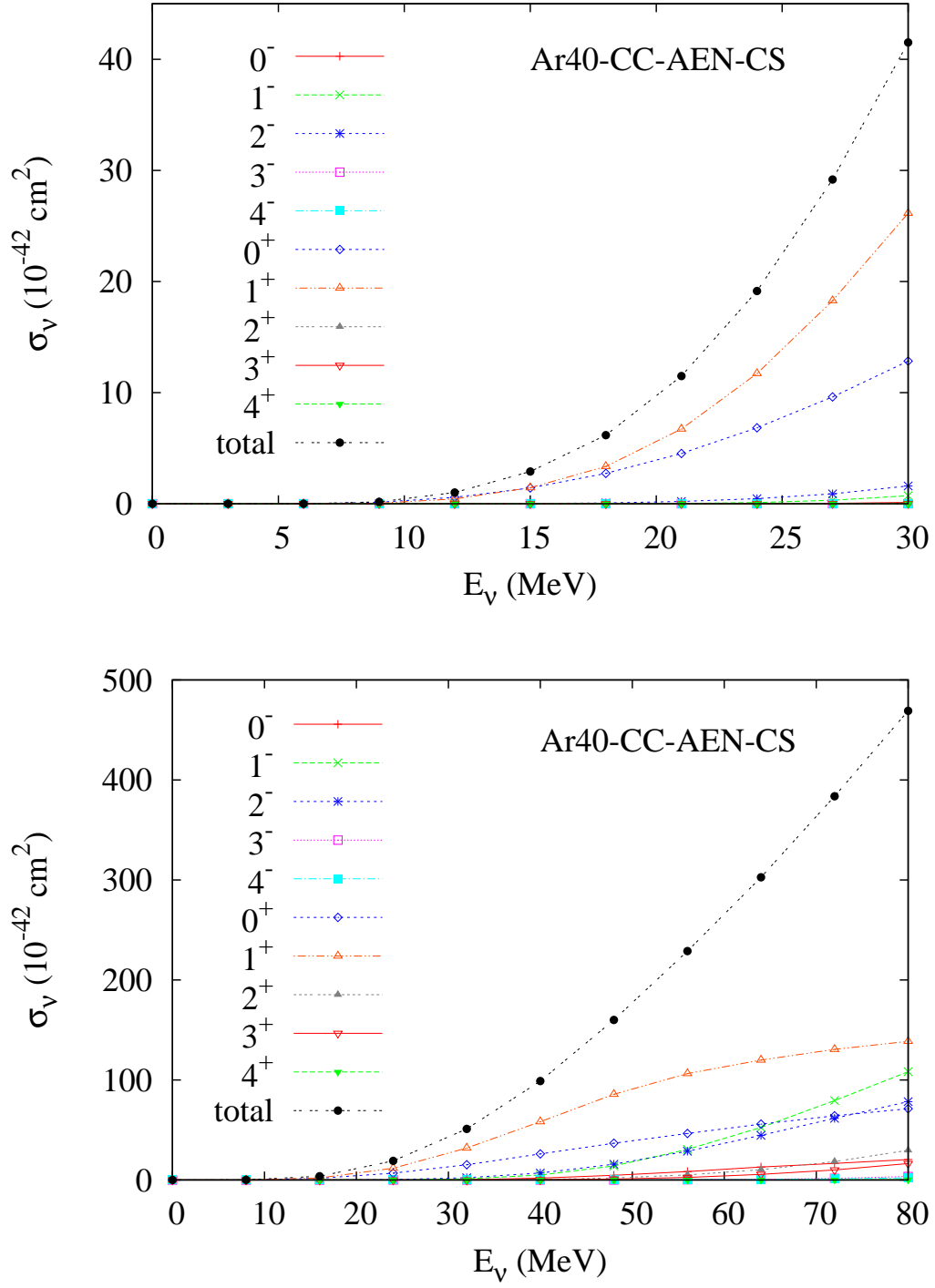


FIG. 3: (Color online) Cross sections by charged current, $^{40}\text{Ar}(\bar{\nu}_e, e^+)^{40}\text{Cl}^*$ for solar (upper) and SN (lower) neutrinos.

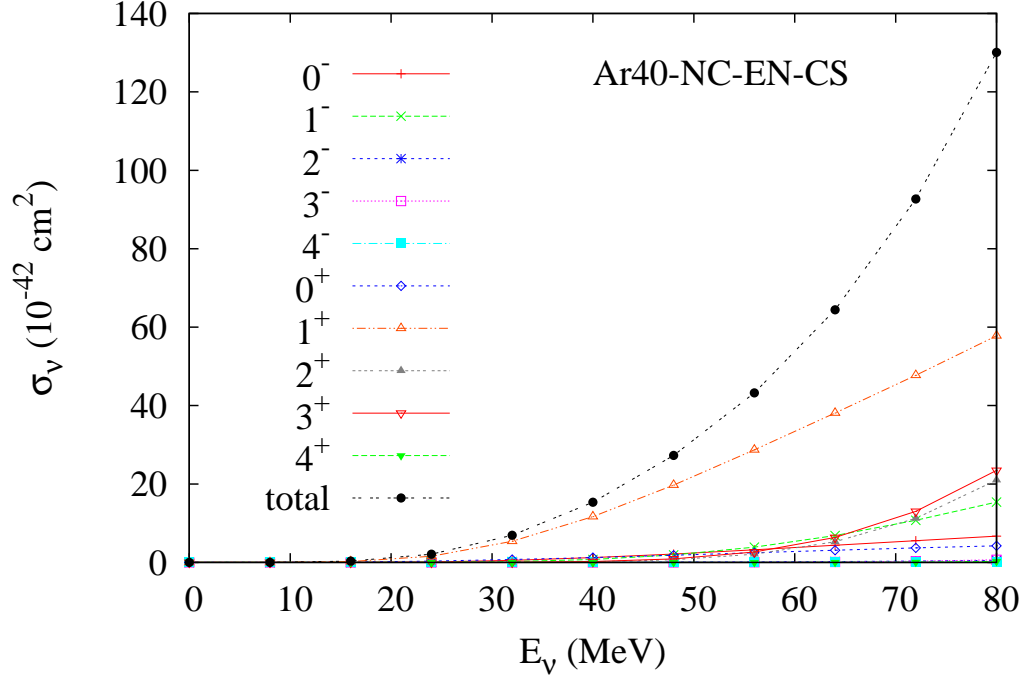
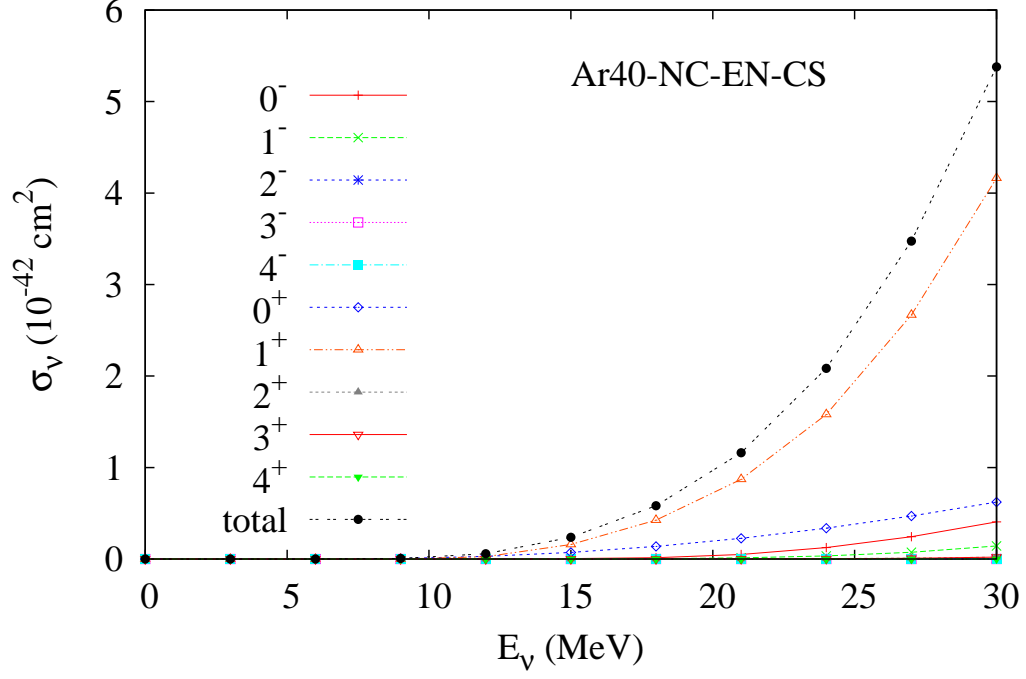


FIG. 4: (Color online) Cross sections by neutral current, $^{40}\text{Ar}(\nu_e, \nu'_e)^{40}\text{Ar}^*$ for solar (upper) and SN (lower) neutrinos.

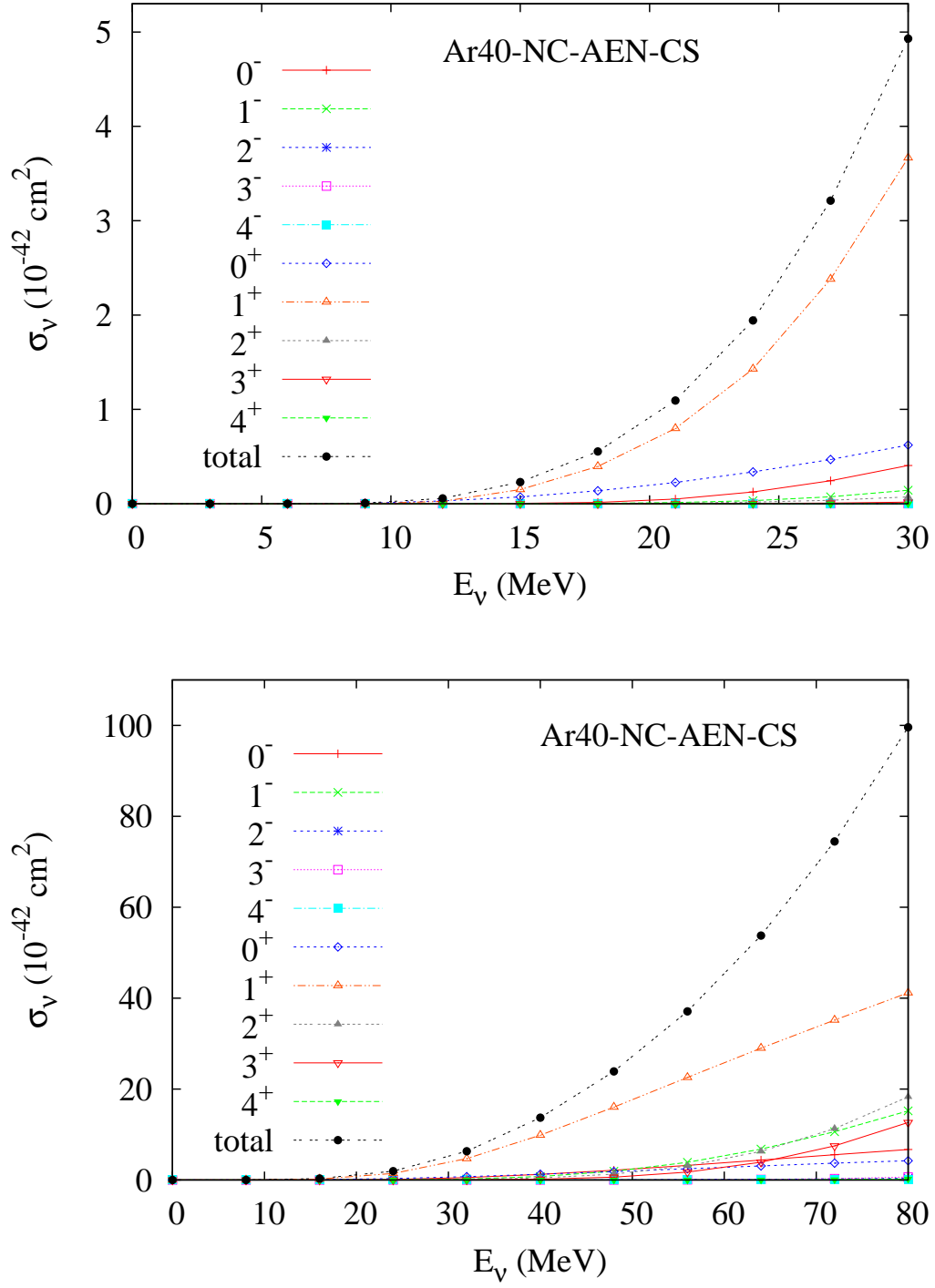


FIG. 5: (Color online) Cross sections by neutral current, $^{40}\text{Ar}(\nu_e, \nu'_e)^{40}\text{Ar}^*$ for solar (upper) and SN (lower) neutrinos.

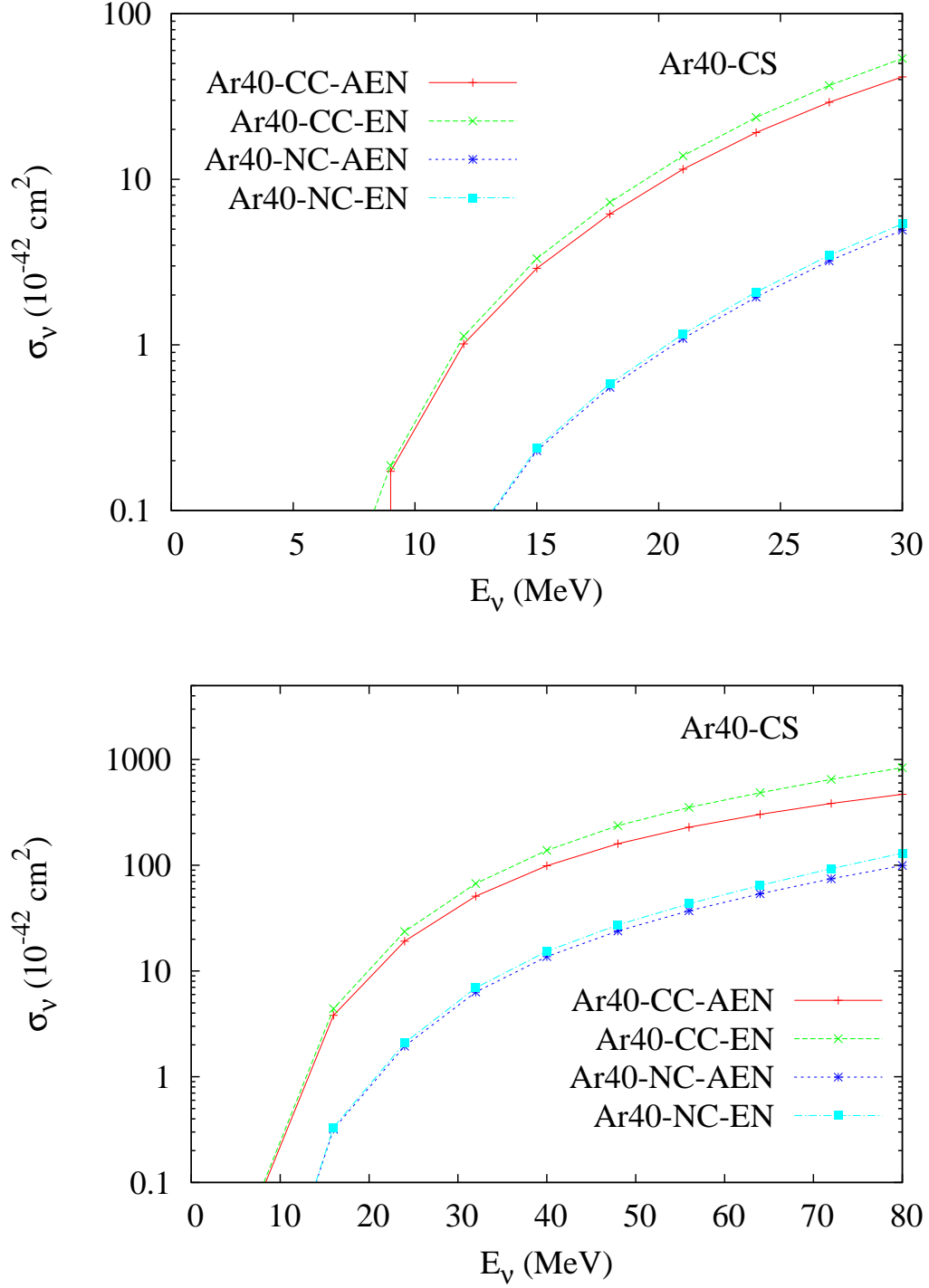


FIG. 6: (Color online) Comparison of cross sections for relevant neutrino reactions on ^{40}Ar given by the log scale for solar (upper) and SN (lower) neutrinos.